Triplet exciton confinement and unconfinement by adjacent hole-transport layers

Kenichi Goushi, Raymond Kwong, Julie J. Brown, Hiroyuki Sasabe, and Chihaya Adachi

---

Triplet exciton confinement and unconfinement by adjacent hole-transport layers

Kenichi Goushi
Department of Photonics Materials Science, Chitose Institute of Science and Technology (CIST), 758-65 Bibi, Chitose, Hokkaido 066-8655 and CREST Program, Japan Science and Technology Agency (JST), Japan

Raymond Kwong and Julie J. Brown
Universal Display Co., 375 Phillips Boulevard, Ewing, New Jersey 08618

Hiroyuki Sasabe and Chihaya Adachi[a)]
Department of Photonics Materials Science, Chitose Institute of Science and Technology (CIST), 758-65 Bibi, Chitose, Hokkaido 066-8655 and CREST Program, Japan Science and Technology Agency (JST), Japan

To understand confinement of the triplet exciton of $Ir(ppy)_3$ by hole-transport layers, we compared energy-dissipative processes of the triplet exciton of $Ir(ppy)_3$ which is doped into 4,4′-bis[N-(1-naphthyl)-N-phenyl-amino]biphenyl (α-NPD), 4,4′-bis [N-(p-tolyl)-N-phenyl-amino]biphenyl (TPD), 1,1-bis[(di-4-tolylamino)phenyl]cyclohexane (TAPC), and 4,4′-N,N′-dicarbazole-biphenyl hosts. Significant energy transfer from $Ir(ppy)_3$ into the triplet levels of α-NPD was observed. In the case of the TPD host, however, partial confinement of the $Ir(ppy)_3$ triplet exciton was observed. This result suggests both forward and backward energy transfer from $Ir(ppy)_3$ to the TPD triplet levels. Furthermore, employing TAPC as a hole-transport layer achieved strong confinement of the $Ir(ppy)_3$ triplet exciton. One conclusion from these results is that electrophosphorescence efficiency is well correlated with the triplet energy level of the hole-transport layer host materials. © *2004 American Institute of Physics.* [DOI: 10.1063/1.1751232]

I. INTRODUCTION

Organic light-emitting diodes (OLEDs) employing iridium (Ir) complexes, specifically (2-phenylpyridine)iridium derivatives, have been demonstrated to have very high efficiency electrophosphorescence.[1–8] Due to the internal heavy-metal effect, these Ir complexes lead to nearly 100% conversion of intersystem crossing (ISC) from singlet to triplet excited states and successively allowance of radiative transitions from the triplet to the singlet ground states. However, to realize this benefit in OLEDs has required further work.

In our study to maximize OLED efficiency, we first must figure out how to confine the triplet excitons of guest molecules by employing host molecules with a high triplet energy level. For example, with OLEDs using the blue phosphor, iridium(III)bis[(4,6-di-fluorophenyl)-pyridinato-N,$C^{2'}$] picolinate (FIrpic), which is doped into 4,4′-N,N′-dicarbazole-biphenyl (CBP), a maximum external quantum efficiency η_{ext} of 6.0% was demonstrated.[5] A rather low η_{ext} of 6.0% of the FIrpic: CBP based OLED is due to a presence of backward energy transfer from the FIrpic triplet level to the CBP triplet level. Further, using the wider-band-gap host 3,5′-N,N′-dicarbazole-benzene (mCP), a higher efficiency ($\eta_{ext}=7.5\%$) of the blue OLED was reported.[6] Most recently, 4,4′-bis(9-dicarbazolyl)-2,2′-dimethyl-biphenyl (CDBP), with a triplet energy of 3.0 eV, demonstrated the highest blue electrophosphorescence efficiency η_{ext} of 10%.[7] Thus, efficient blue electrophosphorescence has been demonstrated by employing emissive exothermic host–guest material combination such as mCP, CDBP, and FIrpic.[8] In a similar manner, various energy-transfer processes from guest to host triplet levels were reported in other articles.[9,10]

In addition to the triplet exciton confinement by host molecules, triplet exciton diffusion into a hole-transport layer (HTL) and an electron transport layer (ETL) should also be considered, since the triplet excitons by charge carrier recombination are usually formed near such interfaces. The loss of energy into the nonradiative decay levels of the HTL and ETL layers can decrease OLED efficiency.

In this study, we investigate triplet energy transfer processes from $Ir(ppy)_3$ into HTLs and identify the requirements for the triplet energy levels of HTLs needed to obtain high electrophosphorescence efficiency. Here, the triplet energy levels were systematically studied by employing four different HTLs including: 4,4′-bis[N-(1-naphthyl)-N-phenyl-amino]biphenyl (α-NPD), 4,4′-bis[N-(p-tolyl)-N-phenyl-amino]biphenyl (TPD), 1,1-bis[(di-4-tolylamino)phenyl]cyclohexane (TAPC), and CBP. Further, the phosphorescent material characteristics were compared with the OLEDs characteristics using a device structure consisting of indium–tin–oxide (ITO)/HTL/7 wt % - $Ir(ppy)_3$: CBP/BCP/Alq_3 /MgAg.

[a)]Author to whom correspondence should be addressed; electronic mail: c-adachi@photon.chitose.ac.jp

II. EXPERIMENT

The α-NPD, TPD, TAPC, and CBP thin films were fabricated by high-vacuum ($\sim 1 \times 10^{-3}$ Pa) thermal evaporation onto a precleaned silicon substrate. Ir(ppy)$_3$-doped hole-transport layers were also prepared by codeposition. The codeposition process was performed by controlling the deposition rate of each evaporation source, independently. The thickness of the organic layers was 50 nm. These films were mounted onto a sample holder using an InGa alloy and then loaded into a cryostat (NAGASE Co., model PS24) for measurement. The phosphorescent spectra of these films were then measured at 5 K. A nitrogen-gas laser with a wavelength λ of 337 nm (Laser Technik Berlin; pulse width: about 500 ps) was used as the excitation source and photoluminescence (PL) transient decay curves were obtained using a streak camera (Hamamatsu Co., C4334).

The OLED devices were fabricated as follows. The organic layers were deposited by high-vacuum (about 1×10^{-3} Pa) thermal evaporation onto precleaned ITO coated glass substrates. The substrate was pre-cleaned by solvent degreasing and ultraviolet–ozone treatment prior to loading into the deposition system. First, a 50-nm-thick HTL was deposited, followed by deposition of a 20-nm-thick light emitting layer (EML) consisting of 7 wt % - Ir(ppy)$_3$ doped CBP. Then the ETL which consisted of a 10-nm-thick 2,9-dimethyl-4,7-diphenyl-1,10-phenanthroline (BCP) and 40-nm-thick tris(8-hydroxyquinoline) (Alq$_3$) were used to confine holes within the EML and inject electrons, respectively. Finally, a shadow mask with 1-mm-diam openings was used to define the cathode consisting of a 100-nm-thick layer of Mg–Ag (10:1) with a 20-nm-thick silver cap layer. We obtained current density (J), voltage (V), and luminance (L) characteristics by using a semiconductor parameter analyzer (Agilent, HP4155C) with an optical power meter (Newport, Model 1835-C).

III. PHOSPHORESCENT SPECTRA OF HOLE-TRANSPORT MATERIALS

All of the hole transport materials (HTMs) (i.e., α-NPD, TPD, TAPC, and CBP) possess negligible phosphorescence at room temperature due to the nonradiative thermal deactivation process from the triplet sates. Since the nonradiative decay can be reduced by a decrease in temperature due to the suppression of molecular vibrations at low temperatures, we were able to detect the phosphorescent spectra of the HTLs at 5 K. Figure 1 summarizes the phosphorescent spectra of α-NPD, TPD, TAPC, and CBP deposited thin films. The triplet energy level (E_T) is estimated from the peaks of the shortest wavelength of the phosphorescent spectra. Compared with E_T of Ir(ppy)$_3$, E_T of α-NPD and TPD resulted in a lower E_T level, whereas E_T of TAPC and CBP resulted in a higher E_T. From these data, we conclude that the triplet exciton confinement of Ir(ppy)$_3$, by these materials, will be significantly different.
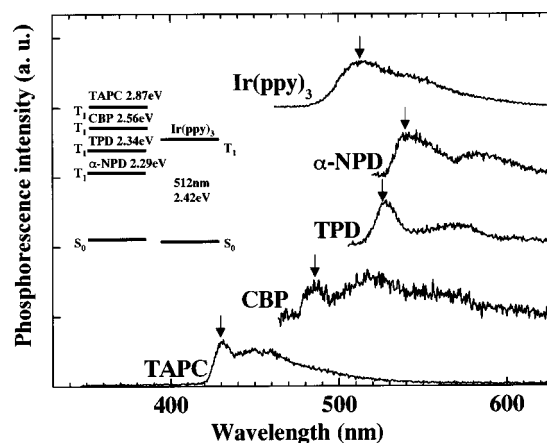

FIG. 1. Phosphorescence spectra of α-NPD, TPD, TAPC, and CBP deposited films and Ir(ppy)$_3$ in a 6 wt % - Ir(ppy)$_3$: CBP film at 5 K. The triplet energy levels of these are also given.

IV. TRIPLET ENERGY CONFINEMENT AND UNCONFINEMENT BY HOLE-TRANSPORT LAYERS

To investigate energy-dissipation processes of Ir(ppy)$_3$ triplet excitons in α-NPD, TPD, TAPC, and CBP, we measured the temperature dependence of the PL transient decay.

Figure 2 compares the PL spectra of the α-NPD film and the 6 wt % - Ir(ppy)$_3$-doped α-NPD film at $T = 5$ K. In the Ir(ppy)$_3$-doped film, we observed the PL emission centered at $\lambda = 541$ nm, which is not the phosphorescent from Ir(ppy)$_3$ but is the phosphorescence of α-NPD. Further, comparing with PL of the α-NPD neat film, the phosphorescence intensity of the α-NPD in the Ir(ppy)$_3$ doped film was significantly enhanced. In addition, the fluorescence intensity of α-NPD decreased in the doped film, and the lifetime ($\tau_f = 0.9$ ns) was shorter than that of the α-NPD neat film ($\tau_f = 2.9$ ns) at $T = 5$ K. Since there is an overlap between α-NPD fluorescence and Ir(ppy)$_3$ absorption in the range of 390–430 nm, energy transfer from the α-NPD singlet into the metal–ligand charge transfer (MLCT) states of Ir(ppy)$_3$ is possible. Here, the lifetime of the α-NPD fluorescence (τ_f) is given by
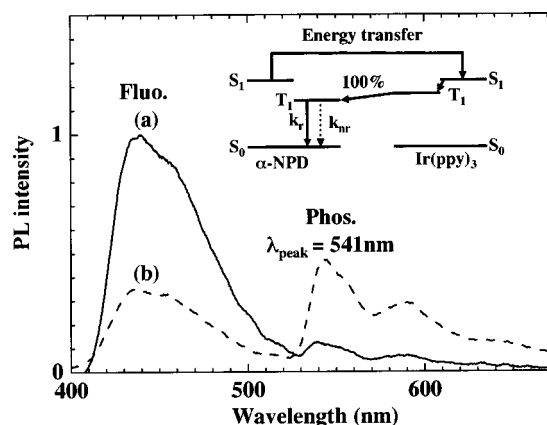

FIG. 2. PL spectra of: (a) α-NPD and (b) 6 wt % - Ir(ppy)$_3$: α-NPD films at 5 K. Also shown are the energy-decay processes in an Ir(ppy)$_3$: α-NPD film. (k_r: radiative transition rate and k_{nr}: nonradiative transition rate). Inset shows energy-transfer mechanism of an Ir(ppy)$_3$: α-NPD film.
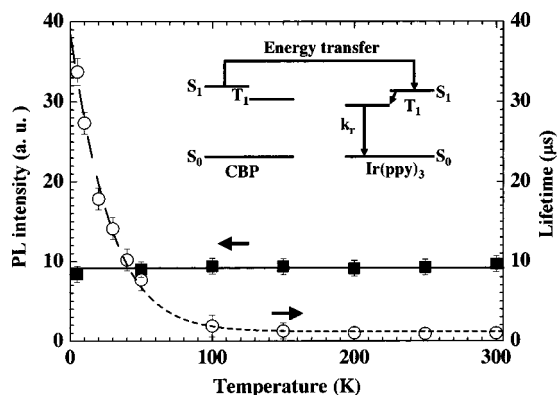
FIG. 3. Temperature dependences of PL intensity (■) and lifetimes (○) for Ir(ppy)$_3$ in 6 wt % - Ir(ppy)$_3$: CBP films. Also shown are the decay processes in the Ir(ppy)$_3$: CBP film.

FIG. 4. Temperature dependences of PL intensity (■) and lifetimes (○) for Ir(ppy)$_3$ in a 6 wt % - Ir(ppy)$_3$: TAPC film. Also shown are the decay processes in the Ir(ppy)$_3$: TAPC film.

$$\tau_f = \frac{1}{k_{rf} + k_{nrf} + k_{isc} + k_{trf}},$$

where k_{rf} is the radiative decay rate from S_1 to S_0, k_{nrf} is the nonradiative decay rate from S_1 to S_0, k_{isc} is the intersystem crossing decay rate from S_1 to T_1, and k_{trf} is the Förster energy transfer rate from α-NPD singlet into the Ir(ppy)$_3$ MLCT levels. In the doped films, k_{trf} is largely due to energy transfer from the α-NPD singlet level into the Ir(ppy)$_3$ MLCT state, while k_{trf} is absent in the neat undoped film. From the difference in the fluorescence lifetimes of doped and undoped films, the Förster energy transfer rate k_{trf} is estimated to be 7.6×10^8. Also, the efficiency of the Förster energy transfer (ϕ_{trf}) is given by

$$\phi_{trf} = \frac{k_{trf}}{k_{rf} + k_{nrf} + k_{isc} + k_{trf}} = k_{trf} \tau_f,$$

where τ_f is the fluorescence lifetime of the doped film. From τ_f of 0.9 ns and k_{trf} of 7.6×10^8, the Förster energy-transfer efficiency ϕ_{trf} is estimated to be 68%. Here, we point out that the α-NPD phosphorescence was significantly enhanced in the doped film. This result suggests that a significant forward energy transfer from the α-NPD singlet level into the Ir(ppy)$_3$ MLCT singlet level occurs after photo-excitation of the α-NPD host layer (inset of Fig. 2). Subsequently, Ir(ppy)$_3$ MLCT singlet excitons convert to the triplet excited states with nearly 100% conversion of ISC. However, Ir(ppy)$_3$ triplet excitons are then transferred back into the α-NPD triplet level (backward energy transfer), because of the lower T_1 level of α-NPD than that of Ir(ppy)$_3$, resulting in enhanced α-NPD phosphorescence.

Figures 3 and 4 show the temperature dependences of PL intensity and lifetime of Ir(ppy)$_3$ in the 6 wt % - Ir(ppy)$_3$: CBP and 6 wt % - Ir(ppy)$_3$: TAPC films, respectively. Interestingly, both PL intensities show no observable temperature dependence. In accordance with these temperature dependences, we observe absolute PL efficiency of these films to be 92% ± 3% in 6 wt % Ir(ppy)$_3$: CBP and 97% ± 3% in Ir(ppy)$_3$: TAPC.[11] Furthermore, the fluorescence of host materials is quenched due to the complete energy transfer from the hosts to the MLCT singlet state of Ir(ppy)$_3$. From these results, in the cases of CBP and TAPC
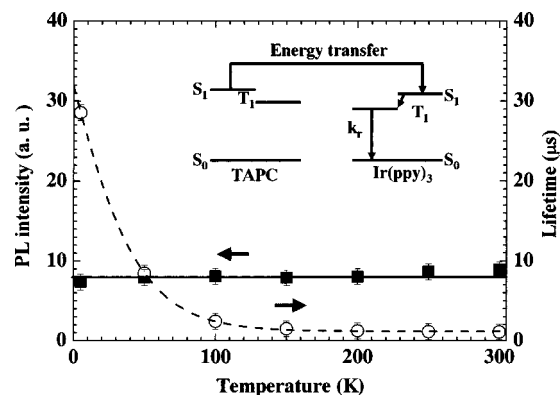
hosts, we conclude that the excited energy is completely transferred to Ir(ppy)$_3$ and that the Ir(ppy)$_3$ triplet excitons decay radiatively with almost 100%. The reason for the unusual luminescence characteristics, where the transient lifetime of Ir(ppy)$_3$ increases significantly at $T < 50$ K, is discussed in detail in a separate article.[12]

Figures 5(a) and 5(b) show the temperature dependences of the transient PL decay and integrated PL intensity for Ir(ppy)$_3$ in the 8 wt % - Ir(ppy)$_3$: TPD films. In this case, phosphorescence intensity of Ir(ppy)$_3$ shows unusual temperature dependences. In addition to the prompt phosphorescence of Ir(ppy)$_3$, the delayed component of Ir(ppy)$_3$ [inset of Fig. 5(a)] is observed. Here, the decay curves can be separated into two single exponential components, suggesting that the phosphorescence decay mechanisms are comprised of two different exciton decay processes. In the prompt phosphorescence of Ir(ppy)$_3$, the energy transfer from the TPD singlet level into the Ir(ppy)$_3$ singlet level occurs after optical excitation of TPD. Subsequently, Ir(ppy)$_3$ singlet excitons decay into the triplet excited state with nearly 100% conversion of the intersystem crossing. Then, because of the competitive triplet energy levels of TPD and Ir(ppy)$_3$, the Ir(ppy)$_3$ triplet excitons decay radiatively to the ground state along with the energy transfer from the Ir(ppy)$_3$ triplet level to the TPD triplet level. Further, the delayed phosphorescence of Ir(ppy)$_3$ is due to the backward energy transfer from the TPD triplet levels into the Ir(ppy)$_3$ triplet level, leading to the delayed Ir(ppy)$_3$ triplet radiative decay. The prolonged lifetime component is thus due to the energy migration between the TPD triplet levels,[9] which retard Ir(ppy)$_3$ phosphorescence emission. Further, the characteristic temperature dependence of PL intensity can be explained by the following mechanism: In comparison to the E_T of Ir(ppy)$_3$ (2.42 eV), the E_T of TPD is slightly lower, i.e., 2.34 eV. Thus, the energy transfer from the TPD triplet level into the Ir(ppy)$_3$ triplet level is endothermic. At temperatures < 150 K, the thermal-activation process from the TPD triplet level to the Ir(ppy)$_3$ triplet level becomes a rate-determining step, therefore the intensity of Ir(ppy)$_3$ phosphorescence is decreased. In addition, the energy transfer from the TPD triplet level into the Ir(ppy)$_3$ triplet level also depends on the nonradiative decay rate of the TPD triplet exciton. The slight
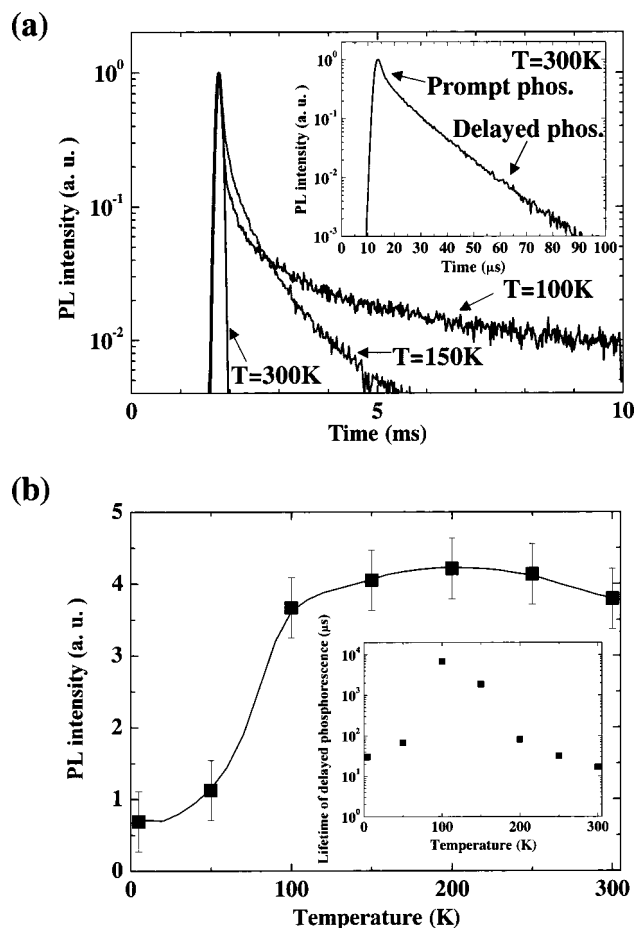
(a)

(b)

FIG. 5. (a) Temperature dependences of the PL decay characteristics for $Ir(ppy)_3$ in 8 wt % - $Ir(ppy)_3$: TPD films. (b) Temperature dependences of the integrated PL intensity for $Ir(ppy)_3$ in a 8 wt % - $Ir(ppy)_3$: TPD film. (Inset) Temperature dependence of the delayed phosphorescence lifetime for $Ir(ppy)_3$ in the 8 wt % - $Ir(ppy)_3$: TPD film.

increase of $Ir(ppy)_3$ phosphorescence for T in the range of 300–200 K is attributed to the suppression of nonradiative decay of the TPD triplet exciton. Due to the suppression, an increase of the backward energy transfer from TPD into $Ir(ppy)_3$ results in enhanced $Ir(ppy)_3$ emission. The increase in the lifetime of the delayed phosphorescence in the range of 300–100 K contributes to the suppression of nonradiative decay of the TPD triplet [inset of Fig. 5(b)]. We thus infer that the $Ir(ppy)_3$ doped TPD film has similar forward and backward triplet energy transfer processes similar to that of the FIrpic:CBP system.[5]

V. OLED CHARACTERISTICS DEPENDING ON HOLE-TRANSPORT LAYERS

Finally, we demonstrate OLED characteristics employing α-NPD, TPD, and TAPC as a HTL. The device structure is an ITO (110 nm)/HTL (50 nm)/7 wt % - $Ir(ppy)_3$: CBP (20 nm)/BCP (10 nm)/Alq_3 (40 nm)/MgAg (100 nm)/Ag (20 nm). Figure 6 shows the external quantum efficiency versus current–density (η_{ext}–J) characteristics of these devices. The OLEDs employing TPD and TAPC as a HTL demonstrated very high η_{ext} of 12% and 14%, respectively, while η_{ext} with α-NPD has been limited to about
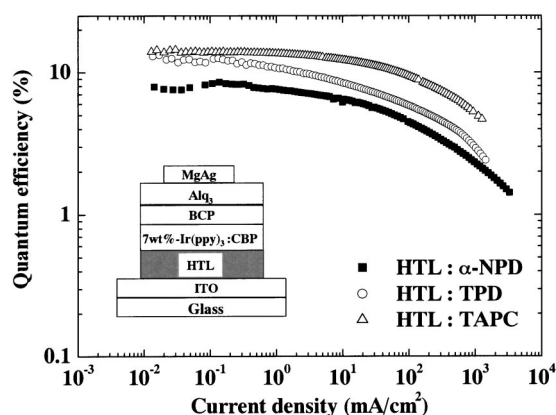

FIG. 6. External quantum efficiency (η_{ext}) vs current density (J) for OLED devices I ($\cdot$) and II ($\cdot$). Device structure I: ITO/TPD (50 nm)/ 7 wt % - $Ir(ppy)_3$: CBP (20 nm)/BCP (10 nm)/Alq_3 (40 nm)/MgAg/Ag. Device structure II: ITO/TAPC (50 nm)/7 wt % - $Ir(ppy)_3$: CBP (20 nm)/BCP (10 nm)/Alq_3 (40 nm)/MgAg/Ag.

8%.[13] We can ascribe these high η_{ext} values to the triplet exciton confinement caused by the HTL. In the OLED with α-NPD as a HTL, the triplet excitons formed on $Ir(ppy)_3$ by carrier recombination partially dissipate into the α-NPD triplet level, leading to a decreased η_{ext}. On the other hand, since the TPD triplet level is slightly higher than that of the α-NPD triplet level, the triplet excitons of $Ir(ppy)_3$ are better confined than those of α-NPD. Furthermore, since the triplet excitons are well confined in the case of a TAPC host, η_{ext} is 14%.

VI. CONCLUSION

In conclusion, the triplet excitons of $Ir(ppy)_3$ are strongly confined in the case of a TAPC host, whereas we demonstrated that the triplet excitons are quenched by an α-NPD host. In the case of TPD, transient PL measurement reveal that the triplet excitons in $Ir(ppy)_3$ are partially confined at room temperature. To achieve high efficiency organic electrophosphorescent diodes, confinement of the triplet exciton of guest molecules by employing a wide-triplet-energy-gap host molecule, which leads to efficient radiative decay of the guest molecule, is critical. Similarly, control of triplet exciton diffusion at the interface of hole transport and emitter layers must also be carefully considered.

[1] M. A. Baldo, S. Lamansky, P. E. Burrows, M. E. Thompson, and S. R. Forrest, Appl. Phys. Lett. **75**, 4 (1999).
[2] C. Adachi, M. A. Baldo, and S. R. Forrest, Appl. Phys. Lett. **77**, 904 (2000).
[3] C. Adachi, M. A. Baldo, M. E. Thompson, and S. R. Forrest, J. Appl. Phys. **90**, 5048 (2001).

[4] C. Adachi, M. A. Baldo, R. C. Kwong, S. Lamansky, M. E. Thompson, and S. R. Forrest, Appl. Phys. Lett. **78**, 1622 (2001).

[5] C. Adachi, R. C. Kwong, P. Djurovich, V. Adamovich, M. A. Baldo, M. E. Thompson, and S. R. Forrest, Appl. Phys. Lett. **79**, 2082 (2001).

[6] R. J. Holmes, S. R. Forrest, Y. J. Tung, R. C. Kwong, J. J. Brown, S. Garon, and M. E. Thompson, Appl. Phys. Lett. **82**, 2422 (2003).

[7] S. Tokito, T. Iijima, Y. Suzuri, H. Kita, T. Tsuzuki, and F. Saito, Appl. Phys. Lett. **83**, 569 (2003).

[8] R. J. Holmes, B. W. D'Andrade, S. R. Forrest, X. Ren, J. Li, and M. E. Thompson, Appl. Phys. Lett. **83**, 3818 (2003).

[9] M. A. Baldo and S. R. Forrest, Phys. Rev. B **62**, 10958 (2000).

[10] F. C. Chen, G. F. He, and Y. Yang, Appl. Phys. Lett. **82**, 1006 (2003).

[11] Y. Kawamura, H. Sasabe, and C. Adachi (unpublished).

[12] K. Goushi, Y. Kawamura, H. Sasabe, and C. Adachi (unpublished).

[13] C. Adachi, R. Kwong, and S. R. Forrest, Org. Electron. **2**, 37 (2001).